Available online at www.sciencedirect.com
SCIENCE DIRECT
Journal of Colloid and Interface Science 284 (2005) 332–338
JOURNAL OF Colloid and Interface Science
www.elsevier.com/locate/jcis

Drag of a dispersion of nonhomogeneously structured flocs in a flow field

Jyh-Ping Hsu [a,*], Ming-Che Li [a], Audrey Chingzu Chang [b]

[a] *Department of Chemical Engineering, National Taiwan University, Taipei, Taiwan 10617*
[b] *Department of Food Science, National I-Lan University, I-Lan, Taiwan 260*

Received 5 August 2004; accepted 21 September 2004

Available online 23 December 2004

Abstract

The influence of floc structure and floc concentration on the drag acting on a floc is investigated theoretically. A two-layer model is adopted to describe floc structure, and a cell model is used to simulate a floc dispersion. The influences of the key parameters of the problem under consideration, including floc concentration, Reynolds number, the ratio (permeability of outer layer/permeability of inner layer), and the ratio (thickness of outer layer/thickness of inner layer), on the drag coefficient are discussed. We show that the more heterogeneous the floc structure is, the greater the drag and the more significant the deviation of curve of variation of drag coefficient against Reynolds number from a Stokes-law-like relation. The drag on a floc declines with the decrease in floc concentration, and, due to the convective flow of the fluid, the distortion of streamlines surrounding a floc becomes more serious and the deviation of the variation of the curve of drag against Reynolds number from a Stokes-law-like relation is more significant.

Keywords: Floc dispersion; Cell model; Nonuniform floc structure; Two-layer model; Drag coefficient

1. Introduction

Flocculation is often observed in natural and industrial processes. Typically, the linear size of the entity formed in flocculation, the so-called floc, ranges from 100 to 1000 μm [1]. Due to its porous nature, floc usually exhibits behavior that is different appreciably from that of rigid entities. In a study of the sedimentation of the floc of activated sludge, Lee et al. [2] found that the Reynolds number can be on the order of 40, which implies that Stokes' law may be inapplicable. The structure of the floc, which depends largely on its formation process, is of a complicated nature. In general, it is irregular in geometry, highly nonuniform, fragile, and permeable, with a porosity higher than 99% [3]. Various floc structures have been proposed, including, for example, homogeneous [1,4–7], three-layered [8], multilayered [9], two-layered with a less permeable outer layer [10], and two-layered with a less permeable inner layer [11]. Hsu and Hsieh [12] considered a two-layered floc structure with various combinations of inner and outer permeability. The following sedimentation problems were analyzed for Reynolds number ranges from 0.1 to 40: a spherical floc in an infinite fluid [12], a spheroidal floc in an infinite fluid [13], a spherical floc along the axis of a cylinder [14], and a spherical floc toward a planar surface [15].

In practice, particles seldom present individually, and a dispersion of multiple particles, that is, a many-body problem, often needs to be considered. In this case, analysis becomes nontrivial even if the problem is solved numerically. Apart from the difficulty arising from solving nonlinear, coupled differential equations, that caused by the complicated nature of the interactions between neighboring particles is also important. The later was circumvented by Happel and Brenner [16] through adoption of a free-surface-cell model, in which a dispersion is simulated by a represented cell comprising a single particle and a concentric liquid shell. Assuming that cells are independent of each other, the drag on a rigid particle in a spherical dispersion was derived under a creeping flow condition. Based on a cell model, Jaiswal

* Corresponding author. Fax: +886-2-23623040.
E-mail address: jphsu@ntu.edu.tw (J.-P. Hsu).

0021-9797/$ – see front matter
doi:10.1016/j.jcis.2004.09.070

et al. [18] analyzed the sedimentation of rigid spheres in a Newtonian fluid numerically. They showed that if the Reynolds number is below 10, the deviation of the friction factor calculated from their correlation relation from that based on Ergun equation is smaller than 10%. This deviation can be larger at a smaller Reynolds number. Under a creeping flow condition, Neale et al. [17] were able to derive an analytical solution for the drag on a uniform floc in a dispersion based on a cell model.

In this study, the drag on a floc in a floc dispersion is evaluated, taking the nonuniform nature of its structure into account. The cell model of Happel and Brenner [16] is adopted to simulate the behavior of a floc dispersion, and a two-layer model used to describe various possible floc structures. The influence of the key parameters such as the concentration of flocs, the Reynolds number, and the permeability and structure of floc on the drag coefficient is discussed.

2. Theory

Referring to Fig. 1, a floc dispersion is simulated by a representative cell, which comprises a floc and a concentric spherical liquid shell of radius R_c. Cylindrical coordinates are adopted with origin at the center of the representative cell, and r and z are respectively the radial and the axial coordinates. r_1 and r_2 are respectively the radii of the outer and the inner layers of a floc, and $\mathbf{V}$ is the bulk velocity of the fluid. The concentration of flocs is estimated by the void fraction ε, defined by

$$\varepsilon = 1 - \left(\frac{r_1}{R_c}\right)^3. \tag{1}$$

We assume that the flow field can be described by [19]

$$\mathbf{u}_f \cdot \nabla \mathbf{u}_f = -\nabla P + \frac{2}{\mathrm{Re}} \nabla^2 \mathbf{u}_f, \tag{2}$$

$$\nabla \cdot \mathbf{u}_f = 0, \tag{3}$$

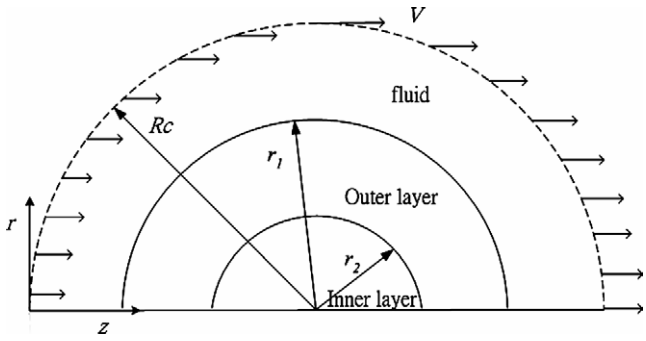

Fig. 1. Schematic representation of the problem considered, where a floc dispersion is simulated by a representative cell, which comprises a floc and a concentric spherical liquid shell of radius R_c. Cylindrical coordinates are adopted with origin located at the center of the representative cell, and r and z are respectively the radial and the axial coordinates. r_1 and r_2 are respectively the radii of the outer and the inner layers of a floc, and $\mathbf{V}$ is the bulk velocity of the fluid.

where $\mathrm{Re} = 2\rho r_1 V_z/\mu$ is the Reynolds number and ρ, μ, and V_z are respectively the density and the viscosity of the fluid and the z-component of $\mathbf{V}$. $P = (p + \rho g Z)/\rho V_z^2$ is the scaled pressure; p, g, and Z are respectively the pressure, gravitational acceleration, and z-coordinate. ∇ is the dimensionless gradient operator, which is scaled by $1/r_1$. $\mathbf{u}_f$ is the dimensionless velocity, which is scaled by $\mathbf{V}$.

Suppose that the flow field inside a floc can be described by the Darcy–Brinkman model and the equation of continuity

$$\mathbf{u}_i + \frac{\mathrm{Re}}{2\beta_i^2} \nabla P = \nabla^2 \mathbf{u}_i, \quad i = 1, 2, \tag{4}$$

$$\nabla \cdot \mathbf{u}_i = 0, \quad i = 1, 2. \tag{5}$$

The subscript i is a region index ($i = 1$ for outer layer and 2 for inner layer of a floc), $\beta_i = r_1/\sqrt{k_i}$ is the scaled floc radius, k_i being the permeability of region i, and $\mathbf{u}_i$ is the scaled flow velocity in region i, which is scaled by $\mathbf{V}$. The boundary conditions associated with Eqs. (2)–(5) are assumed to be

$$u_z = 1, \qquad r = R_c, \tag{6}$$

$$\frac{\partial u_f}{\partial r} = \frac{\partial u_1}{\partial r} = \frac{\partial u_2}{\partial r} = 0, \qquad r = 0, \tag{7}$$

$$\mathbf{u}_f = \mathbf{u}_1 \quad \text{and} \quad \mu_f \nabla \mathbf{u}_f = \mu_1 \nabla \mathbf{u}_1, \qquad r = r_1, \tag{8}$$

$$\mathbf{u}_1 = \mathbf{u}_2 \quad \text{and} \quad \mu_1 \nabla \mathbf{u}_1 = \mu_2 \nabla \mathbf{u}_2, \qquad r = r_2, \tag{9}$$

where u_z is the scaled z-component of the fluid velocity. Equation (7) arises from the symmetric nature of the present problem, and Eq. (8) implies that both the fluid velocity and the shear stress are continuous on the outer layer–liquid interface. The last expression implies that both the fluid velocity and the shear stress are continuous on the boundary of the inner layer–outer layer interface. For simplicity, we assume that $\mu_f = \mu_1 = \mu_2$.

Following the treatment of Neale et al. [17], the drag F on a floc is expressed as

$$F = \left(\frac{1}{2}\rho V_z^2\right)(\pi r_1^2) C_D \Omega, \tag{10}$$

where C_D is the drag coefficient and $\Omega \leqslant 1$ is a correction factor taking account of the porous structure of a floc. For rigid particles, $\Omega = 1$; that is, $F = F_S \Omega$, where F_S is the value of F for the corresponding rigid sphere. For a homogeneously structured floc, Neale et al. [17] were able to derive that, under the condition of creeping flow,

$$\Omega = \frac{2\beta^2[1 - (\tanh\beta/\beta)]}{2\beta^2 + 3[1 - (\tanh\beta/\beta)]}, \tag{11}$$

where $\beta = d_p/2\sqrt{k}$, $d_p = 2r_1$, d_p and r_1 are respectively the diameter and the radius of a floc. In our case, a floc may have a nonuniform structure, and we define the volume-averaged permeability $\bar{k}$ and the scaled radius $\bar{\beta}$ of a floc as

$$\bar{k} = \frac{\sum_{i=1}^{2} V_i k_i}{\sum_{i=1}^{2} V_i}, \tag{12}$$

$$\bar{\beta} = \frac{d_p}{2\sqrt{\bar{k}}}. \tag{13}$$

3. Results and discussion

The governing equations and the associated boundary conditions are solved numerically by FIDAP7.6, a commercial software based on the finite element method. The applicability of this software is examined by comparing the result calculated by it with the analytical result of Happel and Brenner [16] for a dispersion of rigid spheres. Table 1 shows the variation of the percentage error of the former at various combinations of r_1/R_c and ε. As can be seen in this table, the performance of the numerical scheme adopted is satisfactory. The influences of the key parameters of the problem under consideration on both the flow field and the drag coefficient are investigated through numerical simulation in subsequent discussions.

3.1. Variation of flow field

Fig. 2 illustrates the contours for the streamline and the vorticity at various k_1/k_2 at a low Reynolds number for the case when ε is small; that for the case when ε is large is presented in Fig. 3. Here, because both r_1 and $\bar{\beta}$ are fixed, so is the mean permeability of a floc $\bar{k}$, as suggested by Eq. (13). Note that if $k_1/k_2 = 1$, a floc has a uniform structure; if $k_1/k_2 > 1$, the outer layer of a floc is more permeable than its inner layer, and the reverse is true if $k_1/k_2 < 1$. Figs. 2 and 3 suggest that if Re is small, the contours of both streamline and vorticity upstream of a floc are symmetric with those on its downstream. In Fig. 2, ε is small, flocs are close to each other, and the flow field near a floc is influenced appreciably by neighboring flocs. On the other hand, flocs are relatively far apart in Fig. 3, the influence of neighboring flocs is less important, and therefore, the streamlines are less compact than those in Fig. 2. Figs. 2 and 3 also reveal that the results for $k_1/k_2 = 0.1$ are appreciably different from those for $k_1/k_2 = 10$, implying that the influence of floc structure on the flow field is significant even if the mean permeability of a floc is fixed. As Re becomes large, the contours of both streamline and vorticity on upstream of a floc are no longer symmetric to those on its downstream, as can be seen in Figs. 4 and 5. The asymmetric nature of the flow field arises from the presence of convective flow on the downstream of a floc. However, due to the highly porous structure of a floc, either boundary separation or inverse in the direction of fluid velocity are not observed under the conditions assumed. As in the cases of Figs. 2 and 3, the confinement of flow field at a small ε (high floc concentration) is more appreciable than that at a large ε (low floc concentration).

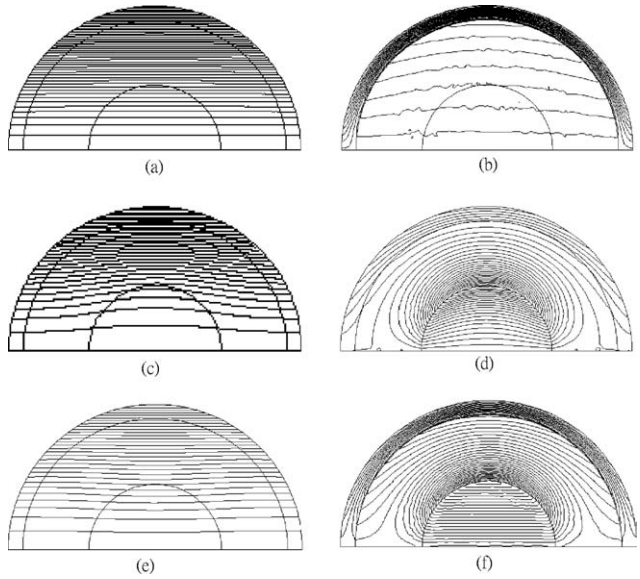

Fig. 2. Contours of streamlines, (a), (c), (e), and vorticity, (b), (d), (f), at various k_1/k_2 for the case when $\varepsilon = 0.271$, Re $= 0.1$, and $\bar{\beta} = 1$. (a) and (b), $k_1/k_2 = 1$; (c) and (d), $k_1/k_2 = 10$; (e) and (f), $k_1/k_2 = 0.1$. Key: $r_1 = 0.12$ cm, $\rho = 1$ g/cm^3, and $\mu = 0.01$ poise.

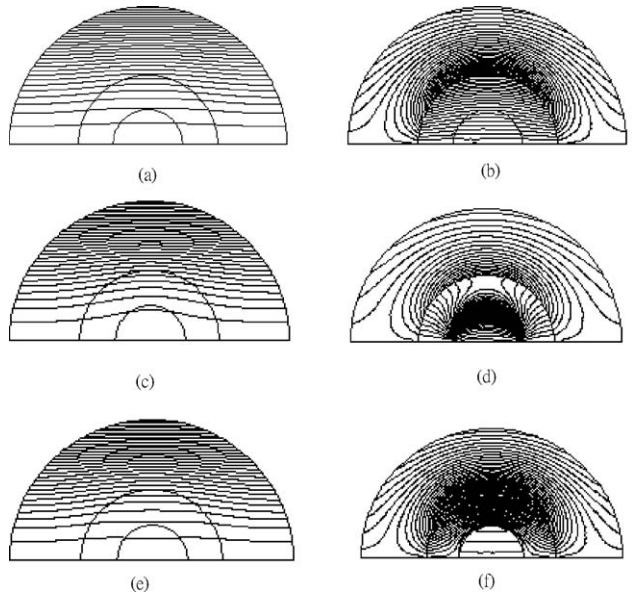

Fig. 3. Contours of streamlines, (a), (c), (e), and vorticity, (b), (d), (f), at various k_1/k_2 for the case of Fig. 2 except that $\varepsilon = 0.875$.

Table 1
Variation of the drag on a rigid sphere at various combinations of r_1/R_c and ε calculated by the analytical result of Happel and Brenner [16] and by the present numerical method

r_1/R_c	ε	Drag $\times 10^4$ (N) [16]	Drag (present) $\times 10^4$ (N)	Percentage error (%)
0.1	0.999	0.1212	0.1198	1.1389
0.3	0.973	0.2425	0.2409	0.6591
0.5	0.875	0.6874	0.6852	0.3335
0.6	0.784	1.4088	1.4035	0.3795
0.7	0.657	3.5654	3.5561	0.2625
0.9	0.271	114.0198	115.9209	−1.6673

Note. Key: $r_1 = 0.12$ cm, $\rho = 1$ g/cm^3, and $\mu = 0.01$ poise.

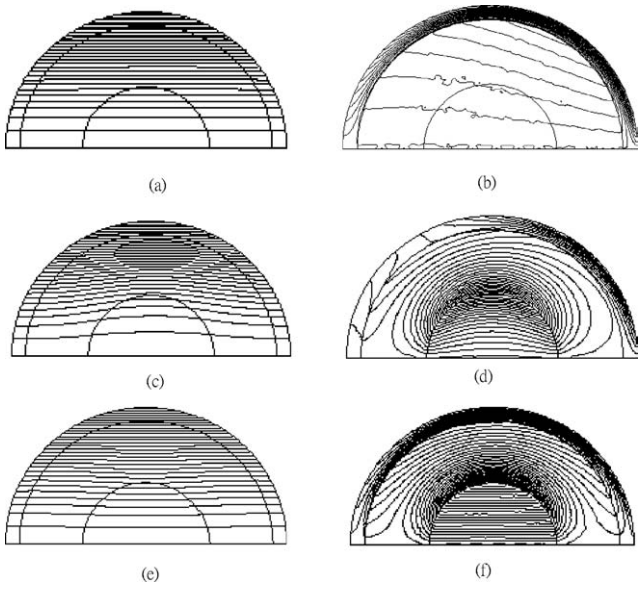

Fig. 4. Contours of streamlines, (a), (c), (e), and vorticity, (b), (d), (f), at various k_1/k_2 for the case when $\varepsilon = 0.271$, Re $= 40$, and $\bar{\beta} = 1$. (a) and (b), $k_1/k_2 = 1$; (c) and (d), $k_1/k_2 = 10$; (e) and (f), $k_1/k_2 = 0.1$. Key: same as in Fig. 2.

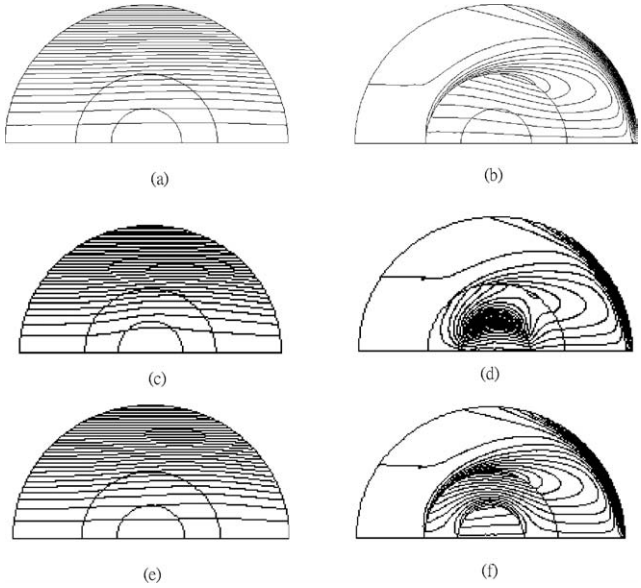

Fig. 5. Contours of streamlines, (a), (c), (e), and vorticity, (b), (d), (f), at various k_1/k_2 for the case of Fig. 4 except that $\varepsilon = 0.875$.

3.2. Effect of floc concentration

The influence of floc concentration on the drag coefficient $C_D\Omega$ at various k_1/k_2 for two different Re is illustrated in Fig. 6. In Fig. 6a Re $= 0.1$, and we have $[C_D\Omega(\varepsilon = 0.271)/C_D\Omega(\varepsilon = 0.999)] = 1.23$, 1.40, 1.29, 1.47, and 1.34 for $k_1/k_2 = 1$, 0.1, 0.2, 10, and 5, respectively. That is, the lower the concentration of flocs, the smaller the drag coefficient, and the more nonuniform the floc structure, the more significant the influence of floc concentration is. Also,

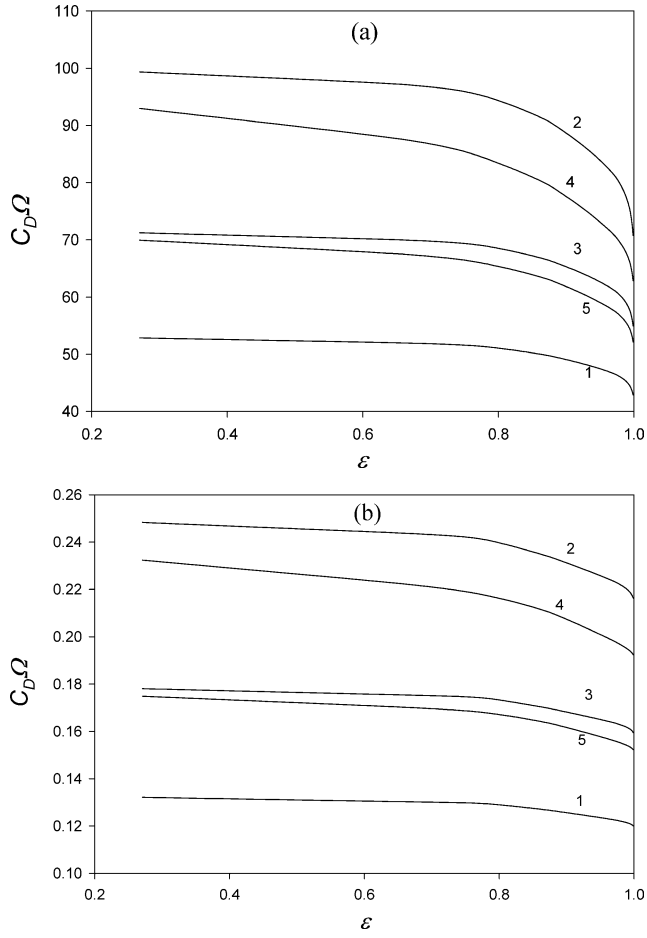

Fig. 6. Variation of $C_D\Omega$ as a function of ε for various k_1/k_2 at different Re for the case when $\bar{\beta} = 1$. Curve 1, $k_1/k_2 = 1$; 2, $k_1/k_2 = 0.1$; 3, $k_1/k_2 = 0.2$; 4, $k_1/k_2 = 10$; 5, $k_1/k_2 = 5$. (a) Re $= 0.1$, (b) Re $= 40$. Key: same as in Fig. 2.

we have $C_D\Omega(k_1/k_2 = 1/10) > C_D\Omega(k_1/k_2 = 10)$ and $C_D\Omega(k_1/k_2 = 1/5) > C_D\Omega(k_1/k_2 = 5)$. That is, for a fixed mean permeability, $C_D\Omega$ is influenced more by the outer layer of a floc than by its inner layer. The general qualitative behavior of $C_D\Omega$ in Fig. 6b is similar to that in Fig. 6a. We have $[C_D\Omega(\varepsilon = 0.271)/C_D\Omega(\varepsilon = 0.999)] = 1.10$, 1.15, 1.12, 1.21, and 1.15 for $k_1/k_2 = 1$, 0.1, 0.2, 10, and 5, respectively. That is, the influence of floc concentration on $C_D\Omega$ becomes less important as Re gets larger.

3.3. Effect of Reynolds number

For creeping flow, the variation of drag coefficient as a function of Reynolds number can be described by the Stokes law [19],

$$C_D = \frac{24}{\mathrm{Re}}. \tag{14}$$

For the present case, this expression can be modified as

$$C_D\Omega = \frac{A(\bar{\beta}, k_1/k_2, \varepsilon)}{\mathrm{Re}}, \tag{15}$$

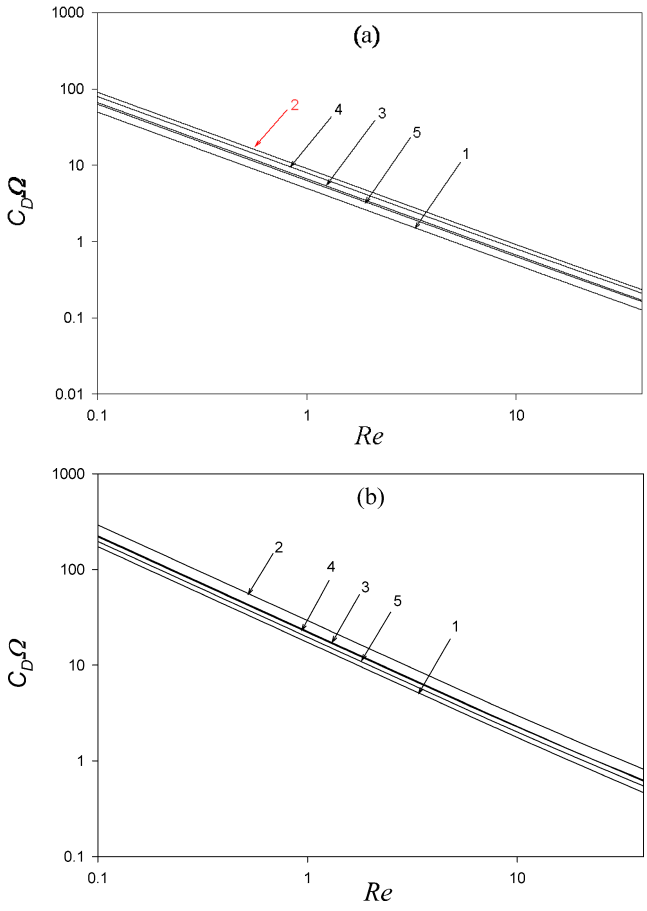

Fig. 7. Variation of $C_D\Omega$ as a function of Re for various k_1/k_2 at different $\bar{\beta}$ for the case when $\varepsilon = 0.875$. Curve 1, $k_1/k_2 = 1$; 2, $k_1/k_2 = 0.1$; 3, $k_1/k_2 = 0.2$; 4, $k_1/k_2 = 10$; 5, $k_1/k_2 = 5$. (a) $\bar{\beta} = 1$, (b) $\bar{\beta} = 2$. Key: same as in Fig. 2.

where A is a function of $\bar{\beta}$, k_1/k_2, and ε. The variations of $\log(C_D\Omega)$ as a function of $\log(\mathrm{Re})$ for various k_1/k_2 at different $\bar{\beta}$ are shown in Fig. 7. Note that the larger the $\bar{\beta}$ the smaller the floc permeability is, and the larger the ε the lower the floc concentration is. Fig. 7 reveals that if Re is small, $\log(C_D\Omega)$ is roughly linearly dependent on $\log(\mathrm{Re})$; that is, a Stokes-law-like relation exists. For rigid spheres, this linear relation is applicable for Re smaller than about 0.1, and for the present flocs, it is applicable for Re two order of magnitudes larger. Fig. 7 also indicates that the larger the $\bar{\beta}$ the more serious is the deviation from the Stokes-law-like relation at large Re. This is because fluid is capable of penetrating through a porous floc, and wakes are relatively hard to form downstream of the floc [20,21]. Table 2 illustrates the percentage deviations from a Stokes-law-like relation at $\mathrm{Re} = 40$ for various combinations of ε and $\bar{\beta}$. This table reveals that at $\varepsilon = 0.271$, because the concentration of floc is high, the convective flow of fluid is confined by neighboring flocs, and the deviation from the Stokes-law-like relation at $\mathrm{Re} = 40$ is negligible. As ε increases to 0.875, the convective flow is appreciable, and the deviation from the Stokes-law-like relation becomes significant.

Table 2
Percentage deviation from Stokes-law-like relation at $\mathrm{Re} = 40$ at various combinations of ε and $\bar{\beta}$

ε	$\bar{\beta}$	k_1/k_2	Percentage deviation (%)
0.875	1	1	1.8206
0.875	1	0.1	3.1649
0.875	1	0.2	2.2009
0.875	1	10	5.7741
0.875	1	5	3.7156
0.875	2	1	7.6123
0.875	2	0.1	11.8642
0.875	2	0.2	9.0782
0.875	2	10	14.6239
0.875	2	5	11.4403
0.271	1	1	0.0022
0.271	1	0.1	−0.0007
0.271	1	0.2	−0.0003
0.271	1	10	0.0062
0.271	1	5	0.0078
0.271	2	1	0.0039
0.271	2	0.1	0.0038
0.271	2	0.2	0.0027
0.271	2	10	−0.0016
0.271	2	5	0.0030

Note. Key: same as in Table 1.

3.4. Effect of mean floc permeability

Fig. 8 shows the influence of the mean floc permeability on the drag coefficient $C_D\Omega$ at various k_1/k_2 for two different Re. As can be seen in this figure, $C_D\Omega$ increases with $\bar{\beta}$; that is, the smaller the mean permeability of floc, or the more rigid its structure, the larger the drag coefficient. Also, $C_D\Omega$ declines with the increase in Re. These results are consistent with the results shown in Figs. 6 and 7. In general, the more nonuniform the structure of a floc the more appreciable is the effect. Note that the curve for $k_1/k_2 = 10$ intersects with that for $k_1/k_2 = 0.2$, implying that there is some interaction between $\bar{\beta}$ and k_1/k_2.

3.5. Effect of floc structure

The simulated variation of $C_D\Omega$ as a function of k_1/k_2 for various combinations of Re and ε is presented in Fig. 9, and that as a function of r_2/r_1 for various k_1/k_2 at different ε is shown in Fig. 10. Fig. 9 reveals that, regardless of the level of floc concentration, the more nonuniform the floc structure is, the larger the drag coefficient, which is consistent with previous observations [12–15]. In general, the more nonuniform the structure of a floc is, the closer its behavior is to that of a rigid floc. Table 3 indicates that the influence of the nonuniform structure of a floc is most important when ε is small and Re is large. According to Eq. (12), for a fixed mean permeability, if $k_1/k_2 < 1$, the increase in r_2/r_1 leads to a less permeable outer layer. On the other hand, if $k_1/k_2 > 1$, the increase in r_2/r_1 leads to a less permeable and relatively thick inner layer. Under both of these conditions the drag coefficient becomes large, as is illustrated in Figs. 10a and 10b. The influence of r_2/r_1 on $C_D\Omega$ is more apprecia-

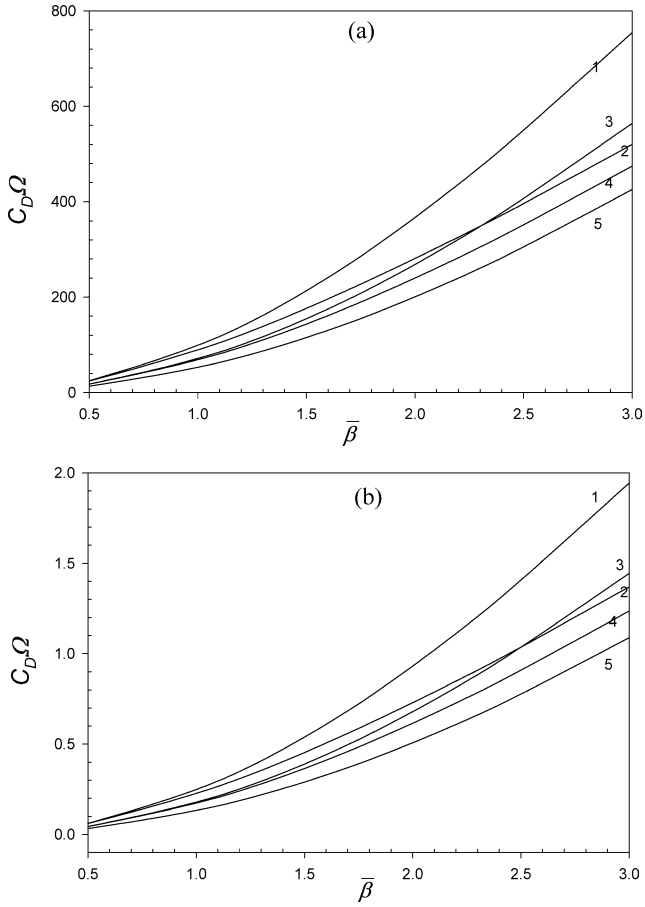

Fig. 8. Variation of $C_D\Omega$ as a function of $\bar{\beta}$ for various k_1/k_2 at different Re for the case when $\varepsilon = 0.657$. Curve 1, $k_1/k_2 = 0.1$; 2, $k_1/k_2 = 10$; 3, $k_1/k_2 = 0.2$; 4, $k_1/k_2 = 5$; 5, $k_1/k_2 = 1$. (a) Re $= 0.1$, (b) Re $= 40$. Key: same as in Fig. 2.

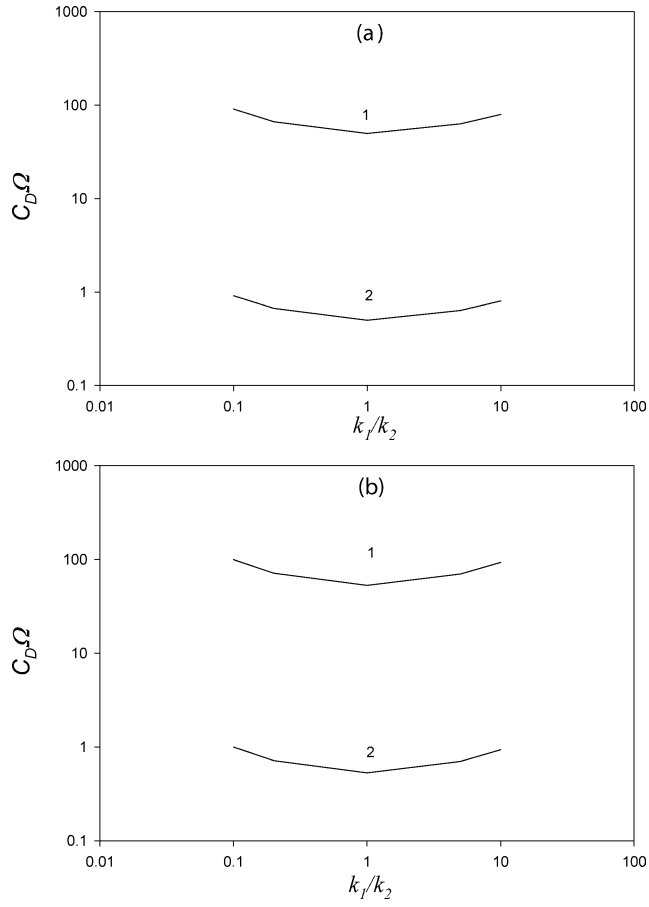

Fig. 9. Variation of $C_D\Omega$ as a function of k_1/k_2 for various combinations of Re and ε for the case when $\bar{\beta} = 1$. Curve 1, Re $= 0.1$; 2, Re $= 40$. (a) $\varepsilon = 0.875$, (b) $\varepsilon = 0.271$. Key: same as in Fig. 2.

ble when floc concentration is lower and/or floc structure is more nonuniform.

4. Conclusion

In summary, the influences of floc structure and floc concentration on the drag acting on a floc are investigated theoretically by adopting a two-layer structural model for the floc and a cell model for floc dispersion. Based on the results of numerical simulations, we conclude the following: (a) If Reynolds number is small, the contours of both streamline and vorticity on the upstream of a floc are symmetric with those on its downstream. They become asymmetric when the Reynolds number is on the order of about 10. If the floc concentration is high, the degree of asymmetry in the flow field as the Reynolds number increases is less appreciable. The influence of floc structure on the flow field is significant even if the mean permeability of a floc remains the same. (b) The lower the floc concentration the smaller is the drag coefficient, and the more nonuniform the floc structure the more significant is the influence of floc concentration. Also, for a fixed mean permeability, the drag coefficient is influenced more by the outer layer of a floc than by its inner layer. The influence of floc concentration on drag coefficient becomes less important as Reynolds number becomes larger. (c) If the Reynolds number is small, a Stokes-law-like rela-

Table 3
Values of $C_D\Omega$ ratios between $k_1/k_2 = 0.1$ and $k_1/k_2 = 1$, and between $k_1/k_2 = 10$ and $k_1/k_2 = 1$ in Fig. 9

ε	Re $= 0.1$	Re $= 40$
0.875	$C_D\Omega(k_1/k_2 = 0.1) = 1.82C_D\Omega(k_1/k_2 = 1)$ $C_D\Omega(k_1/k_2 = 10) = 1.60C_D\Omega(k_1/k_2 = 1)$	$C_D\Omega(k_1/k_2 = 0.1) = 1.83C_D\Omega(k_1/k_2 = 1)$ $C_D\Omega(k_1/k_2 = 10) = 1.61C_D\Omega(k_1/k_2 = 1)$
0.271	$C_D\Omega(k_1/k_2 = 0.1) = 1.88C_D\Omega(k_1/k_2 = 1)$ $C_D\Omega(k_1/k_2 = 10) = 1.76C_D\Omega(k_1/k_2 = 1)$	$C_D\Omega(k_1/k_2 = 0.1) = 1.88C_D\Omega(k_1/k_2 = 1)$ $C_D\Omega(k_1/k_2 = 10) = 1.76C_D\Omega(k_1/k_2 = 1)$

Note. Key: same as in Table 1.

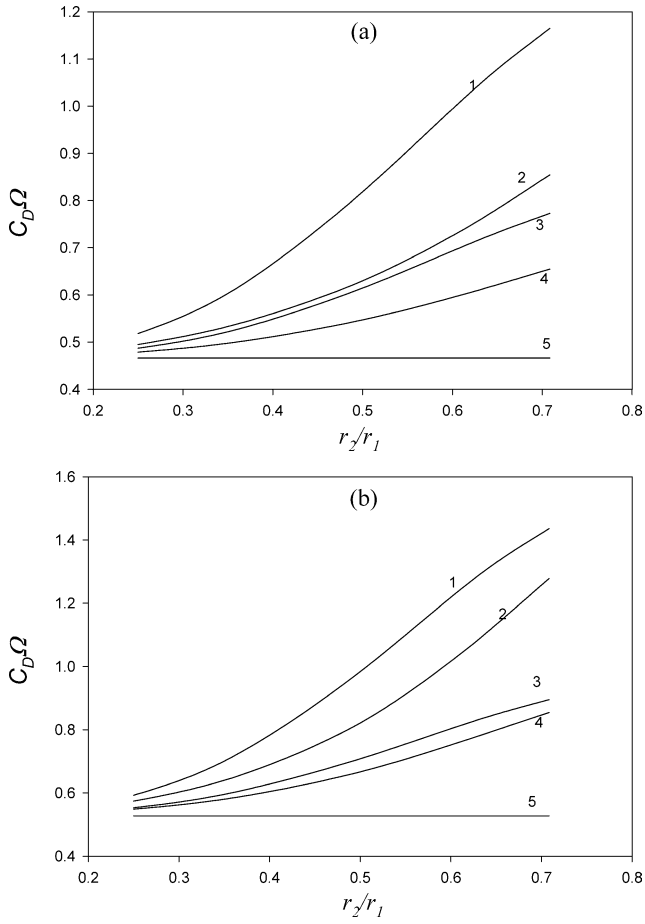

Fig. 10. Variation of $C_D\Omega$ as a function of r_2/r_1 for various k_1/k_2 at different ε for the case when $\bar{\beta} = 2$ and Re $= 10$. Curve 1, $k_1/k_2 = 0.1$; 2, $k_1/k_2 = 10$; 3, $k_1/k_2 = 0.2$; 4, $k_1/k_2 = 5$; 5, $k_1/k_2 = 1$. (a) $\varepsilon = 0.875$, (b) $\varepsilon = 0.271$. Key: same as in Fig. 2.

tion exists. This relation is applicable for Reynolds number two orders of magnitudes larger than that for rigid spheres. The more permeable a floc and/or the higher the concentration of flocs, the easier it is to maintain a Stokes-law-like relation as Reynolds number becomes large. (d) The smaller the mean permeability of the floc, or the more rigid its structure, the larger the drag coefficient. Also, the drag coefficient declines with the increase in Reynolds number, and the more nonuniform the floc structure the more appreciable the effect is. (e) Regardless of the level of floc concentration, the more nonuniform the floc structure, the larger the drag coefficient and the closer its behavior to a rigid floc. The influence of the nonuniform structure of a floc is most important when floc concentration is low and Reynolds number is large. (f) For a fixed mean permeability of a floc, the influence of the relative thickness of the inner layer and the outer layer of a floc on the drag coefficient is more appreciable when floc concentration is lower and/or when the floc structure is more nonuniform.

Acknowledgment

This work is supported by the National Science Council of the Republic of China.

References

[1] C.P. Chu, D.J. Lee, Bull. Coll. Eng. N.T.U. 82 (2001) 49.
[2] D.J. Lee, G.W. Chen, Y.C. Liao, C.C. Hsieh, Water Res. 30 (1996) 541.
[3] C.P. Chu, D.J. Lee, Bull. Coll. Eng. N.T.U. 81 (2001) 47.
[4] R.M. Wu, D.J. Lee, Chem. Eng. Sci. 53 (1998) 3571.
[5] R.M. Wu, D.J. Lee, Chem. Eng. Sci. 54 (1999) 5717.
[6] R.M. Wu, D.J. Lee, Water Res. 35 (2001) 3226.
[7] R.M. Wu, D.J. Lee, Chem. Eng. Sci. 59 (2003) 943.
[8] F. Jorand, F. Zartarian, F. Thomas, J.C. Block, J.Y. Bottero, G. Villemin, V. Urbain, J. Manem, Water Res. 29 (1995) 1639.
[9] S. Veerapaneni, M.R. Wiesner, J. Colloid Interface Sci. 177 (1996) 45.
[10] D.H. Li, J. Ganczarczyk, Biotechnol. Bioeng. 35 (1990) 57.
[11] D.H. Li, J. Ganczarczyk, Water Res. 22 (1988) 789.
[12] J.P. Hsu, Y.H. Hsieh, Chem. Eng. Sci. 57 (2002) 2627.
[13] J.P. Hsu, Y.H. Hsieh, J. Colloid Interface Sci. 259 (2003) 301.
[14] J.P. Hsu, Y.H. Hsieh, J. Colloid Interface Sci. 264 (2003) 517.
[15] J.P. Hsu, Y.H. Hsieh, J. Colloid Interface Sci. 275 (2004) 309.
[16] J. Happel, H. Brenner, Low Reynolds Number Hydrodynamics, Academic Press, New York, 1983.
[17] G. Neale, N. Epstein, W. Nader, Chem. Eng. Sci. 28 (1973) 1865.
[18] A.K. Jaiswal, T. Sundararajan, R.P. Chhabra, Int. J. Eng. Sci. 29 (1991) 709.
[19] R.B. Bird, W.E. Stewart, E.N. Lightfoot, Transport Phenomena, Wiley, New York, 1960.
[20] G.W. Tsou, R.M. Wu, P.S. Yen, D.J. Lee, X.F. Peng, J. Colloid Interface Sci. 250 (2002) 400.
[21] R.M. Wu, D.J. Lee, T.D. Waite, J. Guan, J. Colloid Interface Sci. 252 (2002) 383.